Colloids and Surfaces A 577 (2019) 449–455

Contents lists available at ScienceDirect

Colloids and Surfaces A

journal homepage: www.elsevier.com/locate/colsurfa

Synthesis and self-assembly of chalcone-based organogels

Ying-Peng Zhang*, Bao-Xu Wang, Yun-Shang Yang*, Chuan Liang, Chen Yang, Hong-Li Chai

School of Petrochemical Engineering, Lanzhou University of Technology, Lanzhou 730050, China

GRAPHICAL ABSTRACT

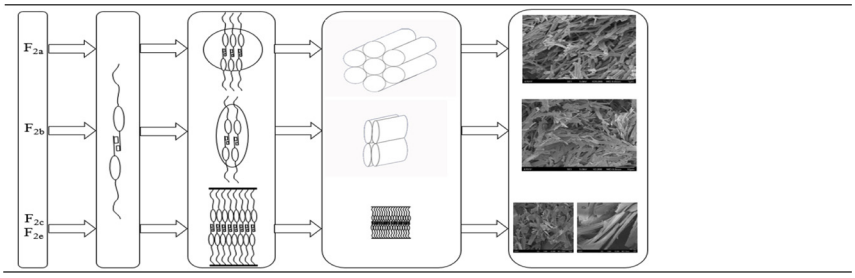

ARTICLE INFO

Keyword:
Naphthalene
Chalcone
Organogels
Alkyl chains
Self-assembly

ABSTRACT

Five naphthalene-type chalcone organogelators with different hydrophobic alkyl units, were designed and synthesized. The prepared organogelators demonstrated excellent gel properties in some selected solvents, such as cyclohexane, *tert*-Butanol, isooctane, and isopropanol etc. The results for thermal stability showed that the alkyl chain length attached to the chalcone also had an important influence on the gelation behavior. Under identical concentrations increasing the length of alkyl chains of the gel molecules and then the gel-to-sol transition temperature value is increased too. It has found that the hydrogen bonding between molecules, the van der Waals force and the π-π stacking provide multiple driving forces for gel self-assembly using various techniques. The morphology of the xerogel was investigated by Scanning Electron Microscope (SEM). As the length of the carbon chain increases, the dry gel tends to form a lamellar network structure. The UV–vis absorption and emission spectra of the gel molecules were also studied.

1. Introduction

Low molecular weight organogels (LMOG) [1–8] are an important class of soft materials that have been synthesized in recent years due to their template synthesis in drug delivery systems, gene therapy, tissue repair, enzyme immobilization, biomedical fields and nanoporous materials. It is important to design a suitable gel molecule, including H bond formation sites and π-π stacking units, including van der Waals forces, electrostatic attraction and hydrophobic interactions necessary for gelation [9–13]. The gel is formed by fractionally assembling a low molecular weight organogel agent into a structure such as "crystal", "belt", "rod" and "tube" in a suitable solvent. In addition to the non-covalent interactions between gel molecules, their affinity for solvent molecules is an important factor in the gelation process. The xerogel helps us better understand the internal structure of the organogels, usually by freeze drying to prepare a xerogel. Low molecular mass organogels have received considerable attention recently on account of their unique features and potential applications for polymeric mesoporous materials [14–16], as templates for silica nanotubes [17], drug delivery [18–20], separations and biomimetics. The self-assembly of such nanoscale supramolecular structures may be important for the production of functional nanomaterials [21–23]. Gel molecules self-

* Corresponding authors.
E-mail addresses: yingpengzhang@126.com (Y.-P. Zhang), yangyunshang@tom.com (Y.-S. Yang).

https://doi.org/10.1016/j.colsurfa.2019.06.010
Received 10 May 2019; Received in revised form 5 June 2019; Accepted 5 June 2019
Available online 06 June 2019
0927-7757/

assemble through highly specific interactions, which allows for preferential one-dimensional growth [24,25]. This one-dimensional growth usually results in the formation of rods, bands or layers. The elongated object is attached to a three-dimensional network of encapsulating solvents to prevent liquid flow.

It has been found that Chalcone itself comprises of two benzene rings linked together by a conjugated enone and does not show any aggregation. They exhibit a broad spectrum of biological activities such as anti-inflammatory [26,27], anti-tuberculosis [28,29], antifungal [30,31], antimalarial [32], anti-leishmanicidal [33], anti-cancer [34–38] and anti-oxidant activity [39–42].

In this work, we synthesized two series of organogel-based compounds based on chalcone units and studied the supermolecule assembly of their molecular structures. We will demonstrate that the introduction of a methoxy group on one side and the introduction of an alkoxy group in the opposite direction results in the aggregation of the resulting molecule and the hydroxyl group of the hydroxychalcone substituted by an alkoxy group in various solvents.

2. Experimental section

2.1. Materials and methods

2-acetyl-6-methoxynaphthalene (98%), *p*-hydroxybenzaldehyde (98.5%), 9-furaldehyde, *n*-octanol, dodecanol, cetyl alcohol, hydrogen bromide was purchased from suppliers. It can be used without further purification. The solvent used for the gelation study was of the AR grade.

2.2. Synthesis of compounds $F_{2a\text{-}2e}$

According to Scheme 1, compounds $F_{2a\text{-}2e}$ comprising a chalcone unit and a long alkoxy chain were prepared as potential organogels. Compound M_1, H_1, H_2 improved synthesis according to literature [43,44]. In the compound $F_{2a\text{-}2c}$, a methoxy group is introduced on one side and an alkoxy group is introduced in the opposite direction; in the compound $F_{2d\text{-}2e}$, a hydroxy group in the hydroxychalcone is substituted with an alkoxy group.

2.2.1. Synthesis of (E)-3-(4-(octyloxy) phenyl)-1-(6methoxynaphthalen-2-yl)prop-2-en-1-one(F_{2a})

Potassium carbonate (4.0 g, 30 mmol) and Potassium iodide (4.0 g, 30 mmol) were added to a solution of M_1 (3.04 g, 10 mmol) in acetone (30 ml) at room temperature. After being stirred for 2 h, M_2 (2.32 g12 mmol) was added dropwise. The reaction mixture was stirred at 80 ℃ for 24 h. After completion of the reaction, it was filtered while hot and the solution was evaporated. The obtained solid was dissolved in chloroform, suction filtered, and the filtrate was washed three times with saturated brine and saturated sodium hydrogen sulfate and dried over anhydrous magnesium sulfate. The crude product was purified by a chromatography column (petroleum ether: ethyl acetate = 30:1) to afford compound F_{2a} (yield: 75%). m.p. 90–93 ℃. ^{1}H NMR (400 MHz, $CDCl_3$): δH ppm 8.46 (s, ArH, 1 H), 8.08 (dd, J = 1.2, 5.6 Hz, ArH, 1H), 7.87 (d, J = 6 Hz, ArH, 1H), 7.84 (d, J = 10.4 Hz, olefinic proton, 1H), 7.80 (d, J = 5.6 Hz, ArH, 1H), 7.62 (d, J = 5.6 Hz, ArH, 2H), 7.56 (d, J = 10.4 Hz, olefinic proton, 1H), 7.20 (dd, J = 1.6, 6 Hz, ArH, 1H), 7.16 (d, J = 1.6 Hz, ArH, 1H), 6.93 (d, J = 5.6 Hz, ArH, 2H), 3.94 (s, 3H), 3.88 (m, overlap, OCH_2, 2H), 1.75–1.49 (t, OCH_2 CH_2, 2H), 1.47–0.92 (m, alkyl chain proton, 10H), 0.91(t, CH_3, 3H). ^{13}C NMR (100 MHz, $CDCl_3$): δ_C ppm 189.9, 161.5, 159.6, 144.4, 137.1, 131.1, 130.2, 129.7, 127.5, 127.2, 125.3119.5, 114.9, 105.8, 77.2, 77.0, 76.8, 70.7, 55.4, 39.3, 30.5, 29.1, 23.8, 23.0, 14.1, 11.1. HR-ESI-MS calculated for $[M+H]^+$ 416.2479, found 417.3089.

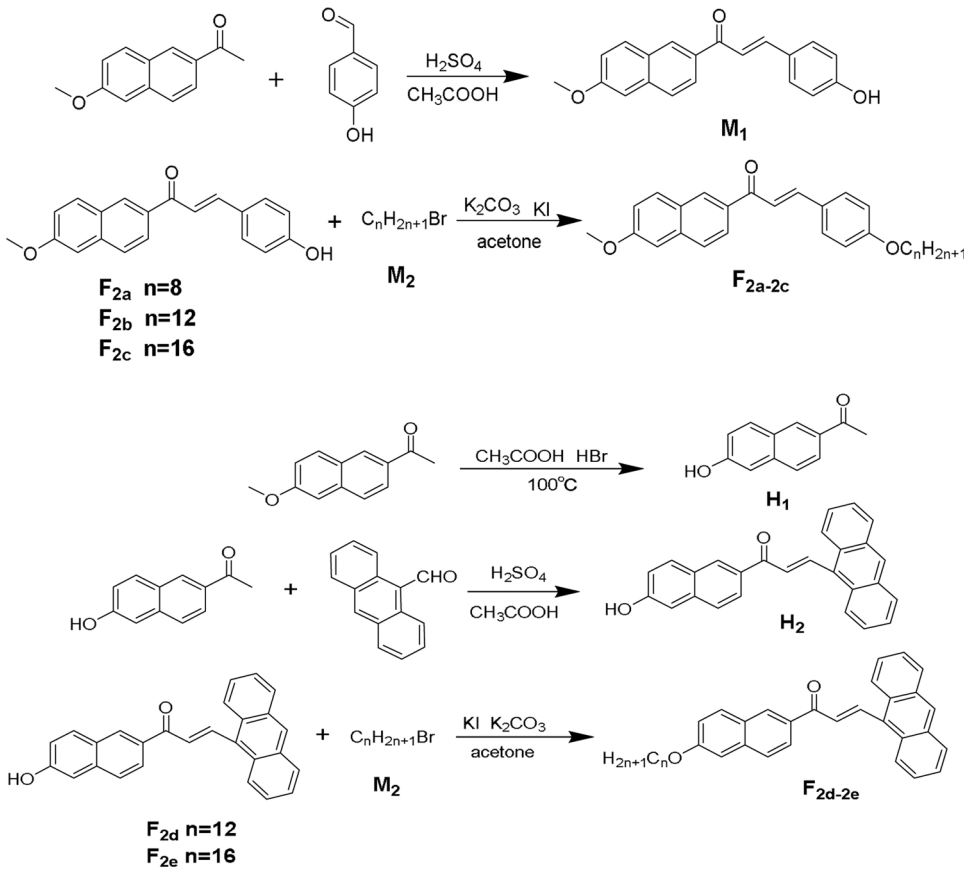

Scheme 1. Synthesis route of chalcone gel molecule $F_{2a\text{-}2e}$.

2.2.2. Synthesis of (E)-3-(4-(dodecyloxy) phenyl)-1-(6-methoxynaphthalen-2-yl)prop-2-en-1-one(F_{2b})

This compound was synthesized by the same procedure described for the synthesis of F_{2a} from M_1 (3.04 g, 10 mmol), Potassium carbonate (4 g, 30 mmol), Potassium iodide (4 g, 30 mmol), M_2 (2.99 g, 12 mmol) in acetone (30 mL) at 80 °C (yield: 71%). m.p. 111–114 °C. ^{1}H NMR (400 MHz, $CDCl_3$): δH ppm 8.46 (s, ArH, 1H), 8.08 (dd, J = 1.2, 5.6 Hz, ArH, 1H), 7.86 (d, J = 6 Hz, ArH, 1H), 7.83 (d, J = 10.4 Hz, olefinic proton, 1H), 7.80 (d, J = 6 Hz, ArH, 1H), 7.61 (d, J = 6 Hz, ArH, 2H), 7.55 (d, J = 10.4 Hz, olefinic proton, 1H), 7.20 (dd, J = 1.6, 6 Hz, ArH, 1H), 7.16 (d, J = 1.6 Hz, ArH, 1H), 6.93 (d, J = 6 Hz, ArH, 2H), 3.99 (m, overlap, OCH_2, 2H), 3.94 (s, 3H), 1.79 (t, OCH_2 CH_2, 2H), 1.47–1.26 (m, alkyl chain proton, 26H), 0.88(t, CH_3, 3H). ^{13}C NMR (100 MHz, $CDCl_3$): δ_C ppm 189.9, 161.3, 159.6, 144.4, 137.1, 131.1, 130.2, 129.7, 127.9, 127.2, 125.3, 119.6, 119.5, 114.9, 105.8, 77.2, 76.9, 76.8, 68.2, 55.4, 31.9, 29.6, 29.6, 29.6, 29.5, 29.4, 29.3, 26.0, 14.1. HR-ESI-MS calculated for $[M+H]^+$ 472.3061, found 473.2963.

2.2.3. Synthesis of (E)-3-(4-(hexadecyl oxy)phenyl)-1-(6-methoxynaphthalen-2-yl)prop-2-en-1-one(F_{2c})

This compound was synthesized by the same procedure described for the synthesis of F_{2a} from M_1 (3.04 g, 10 mmol), Potassium carbonate (4 g, 30 mmol), Potassium iodide (4 g, 30 mmol), M_2 (3.66 g, 12 mmol) in acetone (30 mL) at 80 °C (yield: 75%). m.p. 114–117 °C. ^{1}H NMR (400 MHz, $CDCl_3$): δH ppm 8.46 (s, ArH, 1H), 8.08 (dd, J = 1.2, 5.6 Hz, ArH, 1H), 7.87 (d, J = 5.6 Hz, ArH, 1H), 7.83 (d, J = 10.4 Hz, olefinic proton, 1H), 7.80 (d, J = 5.6 Hz, ArH, 1H), 7.62 (d, J = 5.6 Hz, ArH, 2H), 7.56 (d, J = 10.4 Hz, olefinic proton, 1H), 7.20 (dd, J = 1.6, 6 Hz, ArH, 1H), 7.16 (d, J = 1.6 Hz, ArH, 1H), 6.93 (d, J = 5.6 Hz, ArH, 2H), 4.00 (m, overlap, OCH_2, 2H), 3.95 (s, 3H), 1.80 (t, OCH_2 CH_2, 2H), 1.46–1.26 (m, alkyl chain proton, 26H), 0.88(t, CH_3, 3H). ^{13}C NMR (100 MHz, $CDCl_3$): δ_C ppm 189.9, 161.3, 159.6, 144.4, 137.1, 131.1, 130.2, 129.7, 127.9, 127.2, 125.3, 119.6, 119.5, 114.9, 105.8, 77.2, 76.9, 76.8, 68.2, 63.1, 55.4, 31.9, 29.7, 29.7, 29.6, 29.6, 29.4, 29.4, 26.0, 22.7, 14.1. HR-ESI-MS calculated for $[M+H]^+$ 528.3642, found 529.3498.

2.2.4. Synthesis of (E)-3-(anthracen-9-yl)-1-(6-(dodecyloxy)naphthalen-2-yl)prop-2–en-1-one(F_{2d})

This compound was synthesized by the same procedure described for the synthesis of F_{2a} from H_2 (3.74 g, 10 mmol), Potassium carbonate (4 g, 30 mmol), Potassium iodide (4 g, 30 mmol), M_2 (2.99 g, 12 mmol) in acetone (30 mL) at 80 °C (yield: 75%). m.p. 91–94 °C.^{1}H NMR (400 MHz, $CDCl_3$): δH ppm 8.84 (d, J = 10.4 Hz, olefinic proton, 1H), 8.48 (d, J = 8.8 Hz, ArH, 2H), 8.35 (d, J = 5.6 Hz, ArH, 2H), 8.16 (dd, J = 1.2, 6 Hz, ArH, 1H), 8.03 (d, J = 4.8 Hz, ArH, 2H), 7.81 (d, J = 6 Hz, ArH, 2H), 7.72 (d, J = 10.4 Hz, olefinic proton, 1H), 7.54 (dd, J = 0.8, 4.4 Hz, ArH, 1H), 7.50 (m, ArH, 2H), 7.19 (dd, J = 1.6, 6 Hz, ArH, 1H), 7.16 (d, J = 1.2 Hz, ArH, 1H), 4.10 (m, overlap, OCH_2, 2H), 1.86 (t, OCH_2 CH_2, 2H), 1.52–1.27 (m, alkyl chain proton, 26H), 0.88(t, CH_3, 3H). ^{13}C NMR (100 MHz, $CDCl_3$): δ_C ppm 189.1, 159.5, 131.3, 131.1, 131.1, 130.4, 129.7, 128.9, 127.4, 126.4, 125.4, 125.2, 120.1, 106.5, 77.2, 77.0, 76.8, 68.2, 31.9, 29.7, 29.6, 29.6, 29.6, 29.4, 29.3, 29.1, 26.1, 22.7, 14.1. HR-ESI-MS calculated for $[M+H]^+$ 542.3232, found 543.3232.

2.2.5. Synthesis of (E)-3-(anthracen-9-yl)-1-(6-(hexadecyloxy) naphthalen-2-yl)prop-2-en-1-one (F_{2e})

This compound was synthesized by the same procedure described for the synthesis of F_{2a} from H_2 (3.74 g, 10 mmol), Potassium carbonate (4 g, 30 mmol), Potassium iodide (4 g, 30 mmol), M_2 (3.66 g, 12 mmol) in acetone (30 mL) at 80 °C (yield: 75%). m.p. 126–129 °C.^{1}H NMR (400 MHz, $CDCl_3$): δH ppm 8.84 (d, J = 10.4 Hz, olefinic proton, 1H), 8.48 (d, J = 8.8 Hz, ArH, 2H), 8.35 (d, J = 5.6 Hz, ArH, 2H), 8.16 (dd, J = 0.8, 5.6 Hz, ArH, 1H), 8.03 (d, J = 5.2 Hz, ArH, 2H), 7.81 (d, J = 6 Hz, ArH, 2H), 7.72 (d, J = 10.4 Hz, olefinic proton, 1H), 7.54 (dd, J = 0.8, 4.4 Hz, ArH, 1H), 7.50 (m, ArH, 2H), 7.19 (dd, J = 1.6, 6 Hz, ArH, 1H), 7.16 (d, J = 1.6 Hz, ArH, 1H), 4.09 (m, overlap, OCH_2, 2H), 1.86 (t, OCH_2 CH_2, 2H), 1.50–1.26 (m, alkyl chain proton, 26H), 0.88(t, CH_3, 3H). ^{13}C NMR (100 MHz, $CDCl_3$): δ_C ppm 189.1, 159.5, 141.4, 131.3, 131.1, 130.4, 129.7, 128.9, 127.4, 126.4, 125.4, 125.2, 120.1, 106.5, 77.2, 77.0, 76.8, 68.2, 31.9, 29.7, 29.7, 29.6, 29.6, 29.5, 29.4, 29.3, 26.1, 22.7, 14.1. HR-ESI-MS calculated for $[M+H]^+$ 598.3876, found 599.4378.

2.3. Gelation test

Weigh 0.0025 g of compound $F_{2a\text{-}2e}$, put it into a small reagent bottle [3 cm (height) × 0.5 cm (radius)], and add 0.25 ml of organic solvent (corresponding concentration is 1%, g/ml) under closed conditions. It was completely dissolved by heating, and after standing, it was cooled to room temperature. Invert the cooled glass bottle and observe the solution flow. If the solution does not flow, it means that the solution forms a gel during the cooling process, denoted as G; if the solution and solid coexist, it means that part of the gel is formed and recorded as PG; after cooling to room temperature, it is still a solution, expressed as S. The gel forming solvent was further measured to determine the minimum gel concentration [45].

2.4. Characterizations

^{1}H NMR and ^{13}C NMR spectra were measured on a Bruker Avance 400 (400 MHz) spectrometer using deuterated chloroform ($CDCl_3$) as solvent and using tetramethylsilane (TMS) as an internal standard. ^{1}H and ^{13}C NMR chemical shifts were reported relative to TMS. The coupling constant (J) is expressed in Hz and the chemical shift (d) is expressed in ppm. SEM images were recorded on JSM-6701F cold field emission scanning electron microscope. X-ray diffraction (XRD) patterns were recorded by Bruker Xps GADDS. HRMS spectra were recorded on the Bruker Daltonics Esquire 6000. FT-IR spectra were recorded on the Fourier Transform Infrared Spectrometer from Nicolet, USA. Scanning electron microscope (SEM) were recorded by JSM-670F.

3. Results and discussion

3.1. Synthesis

Compound $F_{2a\text{-}2e}$ was prepared as a potential organogel according to Scheme 1, and all compounds were verified by ^{1}H RMS, ^{13}C RMS and HRMS to confirm the correct structure.

3.2. Gelation study

The experimental results are shown in Table 1. As can be seen from Table 1, the compounds $F_{2a\text{-}2c}$ can form a gel in alcohols, alkanes and acetone. F_{2d} does not form a gel in any solvent, F_{2e} can only form a gel in alcohols, and there is no gelation ability in other solvents. This may be related to the position at which the alkoxy group is located. When the alkoxy group is located on the benzene ring in the chalcone unit, it exhibits good gelation ability, for example, $F_{2a\text{-}2c}$; However, when the alkoxy group is located on the naphthalene ring in the chalcone unit, it has no gelling ability, for example, F_{2d}; when the alkoxy chain is long, it exhibits a weak gelling ability such as F_{2e}. Therefore, the melting temperature of the compound $F_{2a\text{-}2e}$ was further investigated.

3.3. Transition temperatures study

Table 2 lists the solubilization temperatures of the compounds $F_{2a\text{-}2e}$ in the gel-solution phase transition. As can be seen from the table, the compound $F_{2a\text{-}2c}$ as a whole exhibit a tendency to increase in temperature, because as the alkyl chain grows, the gel becomes more and more stable, so the temperature tends to increase. The gel molecule F_{2c}

Table 1
Gelation test results of compound $F_{2a\text{-}2e}$ (1%).

Solvent	result				
	F_{2a}	F_{2b}	F_{2c}	F_{2d}	F_{2e}
ethanol	PG	PG	G	S	PG
iso-propanol	G	PG	PG	PG	G
tert-butanol	G	G	PG	PG	G
n-butanol	S	G	G	PG	G
n-pentanol	PG	G	G	PG	G
n-heptane	G	G	PG	PG	PG
isooctane	G	G	G	PG	PG
acetone	S	G	S	S	S
ethyl acetate	S	S	S	S	S
ethyl acetoacetate	S	PG	S	S	PG
cyclohexane	G	PG	PG	S	S
diethyl malonate	S	S	S	S	S
dichloromethane	S	S	S	PG	S
chloro-*n*-butane	S	PG	S	S	S
tert-amyl alcohol	PG	PG	PG	S	S

S = solution; G = gel; PG = partial gel. Critical gelation concentration (CGC) is presented in parentheses [% (w/v)].

Table 2
Compound $F_{2a\text{-}2e}$ transition temperature.

Solvent	T_{gel} (°C)				
	F_{2a}	F_{2b}	F_{2c}	F_{2d}	F_{2e}
ethanol	/	/	80 °C	/	/
iso-propanol	66 °C	/	/	/	90 °C
tert-butanol	65 °C	84 °C	/	/	82 °C
n-butanol	/	75 °C	85 °C	/	86 °C
n-pentanol	/	75 °C	82 °C	/	83 °C
n-heptane	63 °C	77 °C	/	/	/
isooctane	68 °C	63 °C	85 °C	/	/
acetone	/	82 °C	/	/	/
cyclohexane	73 °C	/	/	/	/

has the same long alkyl chain as F_{2e}. Since the conjugation of the chalcone structure in the gel molecule F_{2e} is more stable, the gel molecule F_{2e} has a higher melting temperature.

As can be seen from the table, F_{2a} is in cyclohexane; F_{2b} is in *tert*-butanol; F_{2c} is in isooctane; F_{2e} *iso*-propanol is relatively high in temperature.

The gel formed by the gel molecule $F_{2a\text{-}2c}$ in an organic solvent is shown in Fig. 1, where in the gel formed by F_{2b} in a *tert*-butanol solvent is a pale-yellow gel; the gels formed by F_{2a} is in cyclohexane and F_{2c} in isooctane were all white gels. Fig. 2 is a gel-solution phase transition diagram of the F_{2e}-*iso*-propanol system. Taking these four gels as examples, we examined some basic properties of the gel.

3.4. Fluorescence performance study

Because gel molecules have potential application value in the fields of fluorescent switches and sensors. So, we further explored the fluorescent properties of compound $F_{2a\text{-}2c}$. Fig. 3 shows the UV absorption

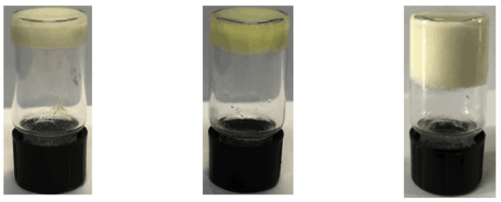

Fig. 1. F_{2a}-cyclohexane, F_{2b}-*tert*-butanol, F_{2c}-isooctane gel diagram.

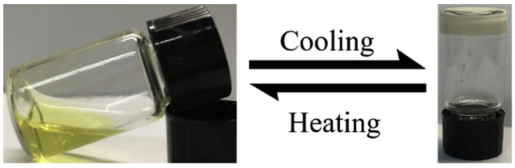

Fig. 2. Gel-sol conversion diagram of gel molecule F_{2e}-*iso*-propanol.

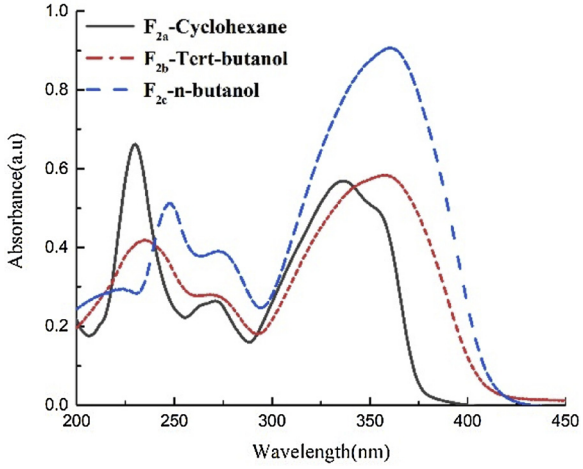

Fig. 3. UV absorption spectrum of F_{2a}-cyclohexane, F_{2b}-*tert*-butanol and F_{2c}-n-butanol.

spectra of F_{2a}-cyclohexane, F_{2b}-*tert*-butanol, and F_{2c}-n-butanol. The cyclohexane solution of F_{2a} has a strong absorption peak at 230 nm, 271 nm, and 335 nm, and in the ultraviolet spectrum of F_{2b}-*tert*-butanol and F_{2c}-n-butanol system, the positions of the peaks are red-shifted to different degrees, and the peaks at 335 nm are red-shifted to 357 nm and 361 nm, respectively. This red shift may be related to the length of the alkyl chain introduced.

In the fluorescence spectrum, the fluorescence intensity of the F_{2a}-cyclohexane solution gradually decreased with the increase of the concentration until the final gradual but no red shift, indicating that in the solution system, the molecular collision degree increases, resulting in fluorescence intensity. When the concentration of F_{2b}-*tert*-butanol system increases, the emission peak shifts from 410 nm to 440 nm, and the fluorescence quenches, indicating that the gel molecule π system is enhanced, and π-π occurs during gel formation (Fig. 4).

3.5. Fourier Transform Infrared Spectrometer (FT-IR) studies

To confirm the presence of intermolecular hydrogen bonds in the system, F_{2a}-cyclohexane xerogel, F_{2b}-*tert*-butanol xerogel, F_{2c}-isooctane xerogel and F_{2e}-*iso*-propanol xerogel were tested by FT-IR spectroscopy. The molecular characteristic absorption signals in the monodispersed state are: C—H stretching vibration peak appears at about 3000 cm^{-1}, C═O double bond stretching vibration appears at around 1690 cm^{-1}, and C—O bond stretching vibration appears at 1250 cm^{-1}. As shown in Fig. 5, the C—H stretching vibrations in the four samples $F_{2a\text{-}2c}$ and F_{2e} (in order of 2923 cm^{-1}, 2922 cm^{-1}, 2920 cm^{-1}, 2920 cm^{-1}) and the stretching vibration of C═O double bond (in order of 1623 cm^{-1}, 1616 cm^{-1}, 1614 cm^{-1}, 1620 cm^{-1}), the absorption peaks move in the direction of decreasing wave number. The stretching vibration of the C—O bond (in order of 1254 cm^{-1}, 1261 cm^{-1}, 1257 cm^{-1}, and 1266 cm^{-1}) shifts in the direction of increasing wave number. These movements indicate intermolecular hydrogen in the gel molecule. Based on the structure of the molecule, it is inferred that the gel molecules may form aggregate structures primarily by self-assembly of intermolecular hydrogen bonding and van der Waals forces between the alkyl chains. At the same time, it can be seen from the absorption

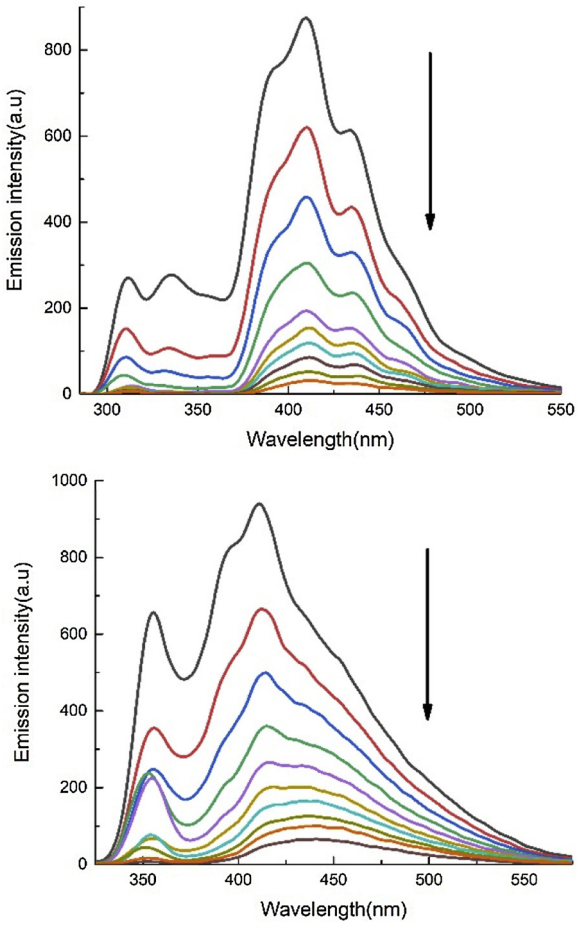

Fig. 4. Fluorescence titration of F_{2a}-cyclohexane and F_{2b}-*tert*-butanol.

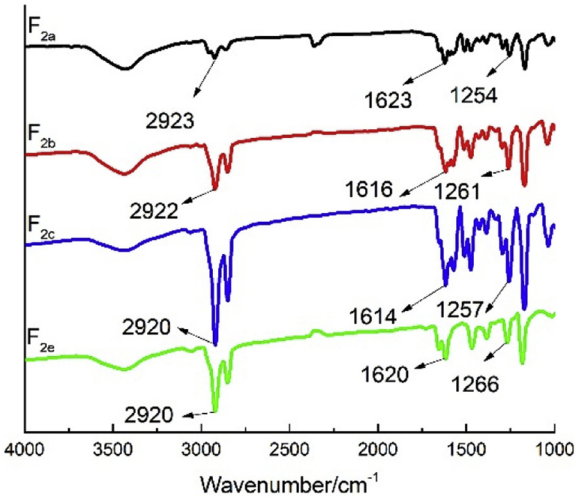

Fig. 5. Infrared spectrum of chalcone gel molecule $F_{2a\text{-}2c}$ and F_{2e} xerogel.

intensity of $F_{2a\text{-}2c}$ that as the alkyl chain grows, the absorption intensity increases, indicating that the longer the alkyl chain, the greater the intermolecular hydrogen bonding.

3.6. X-ray diffraction (XRD) studies

The powdered X-ray diffraction was used to analyze the accumulation of gel molecules $F_{2a\text{-}2c}$ xerogels and F_{2e} xerogel as shown in Fig. 6: F_{2a}-cyclohexane xerogel sample in the small corner area

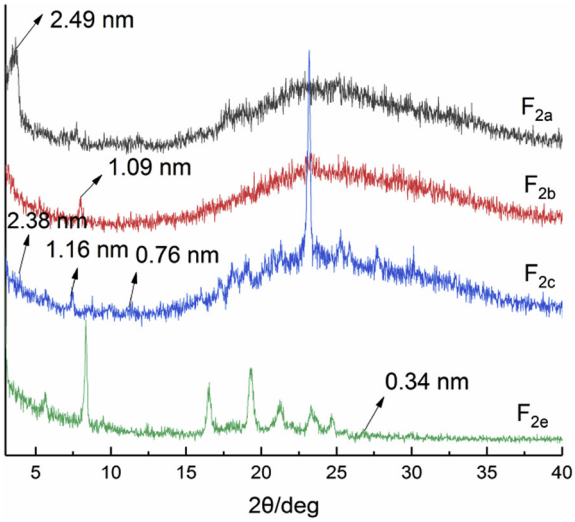

Fig. 6. XRD spectra of chalcone gel molecule $F_{2a\text{-}2c}$ and F_{2e} and xerogel.

$2\theta = 3.5^{\circ}$(2.49 nm) has a strong diffraction peak, indicating that the F_{2a} xerogel molecule is fully extended in the gel, and a wide diffraction peak in the wide-angle region, indicating that the alkyl chains are disorderly stacked up. The accumulation of gel molecules is loose, which may be due to the disordered stacked up of the alkyl chains weakening the Intermolecular hydrogen bonding, resulting in a looser stacked up. The diffraction peak of F_{2b}-*tert*-butanol xerogel disappears in the wide-angle region, and becomes a large peak package, indicating that the arrangement of molecules is relatively disordered. However, there are several spikes in the small-angle region, indicating that based on intermolecular hydrogen bonds is relatively tight, which is significantly different from the way in which F_{2a} molecules are stacked. The F_{2c}-isooctane xerogel sample exhibited many sharp diffraction peaks, indicating that the aggregate structure in the gel was tightly packed. Three higher diffraction peaks can be seen from the figure, and the corresponding d values are 2.38 nm, 1.16 nm, 0.76 nm, in accordance with (1/1): (1/2): (1/3), indicating that the xerogel molecules are layered stacked to approximate the crystalline structure, which is also related to the results obtained by SEM were consistent. The F_{2e}-*iso*-propanol xerogel sample has a strong diffraction peak at $2\theta = 8.3^{\circ}$ in the small corner region, indicating a fully extended conformation in the xerogel, and many sharp diffraction peaks in the wide-angle region, it shows that the aggregate structure in the gel is tightly packed, which is similar to the crystalline structure, which is also consistent with the results observed by SEM. From the diffraction pattern of the F_{2e}-*iso*-propanol xerogel, it can be seen that the corresponding d value is 0.34 nm at $2\theta = 26.64^{\circ}$. It was shown that a π-π stacking occurred between the naphthalene rings in the molecular structure of the gel.

3.7. Scanning electron microscope (SEM) studies

The microscopic morphology of the dry gel formed by chalcone organogel in different solvents was observed by cold field scanning electron microscopy. The result is shown in Fig. 7, as can be seen from the figure, the gel molecule F_{2a} forms a micro-scale rod-like structure in a cyclohexane solvent. These rod-like structures are entangled with each other through a plurality of nodes to form a stable spatial network structure and form stable gel together with cyclohexane. The gel molecule F_{2b} forms a regular band-like structure in *tert*-butanol, when it is magnified 2000 times, a relatively complete spatial network structure can be seen; when the magnification is 10,000 times, it can be seen that these band-like stacks are Tighter. The gel molecule F_{2c} tends to form a lamellar structure in an isooctane solvent, but belongs to an irregular lamellar structure, and the aggregate structure is closely packed, which

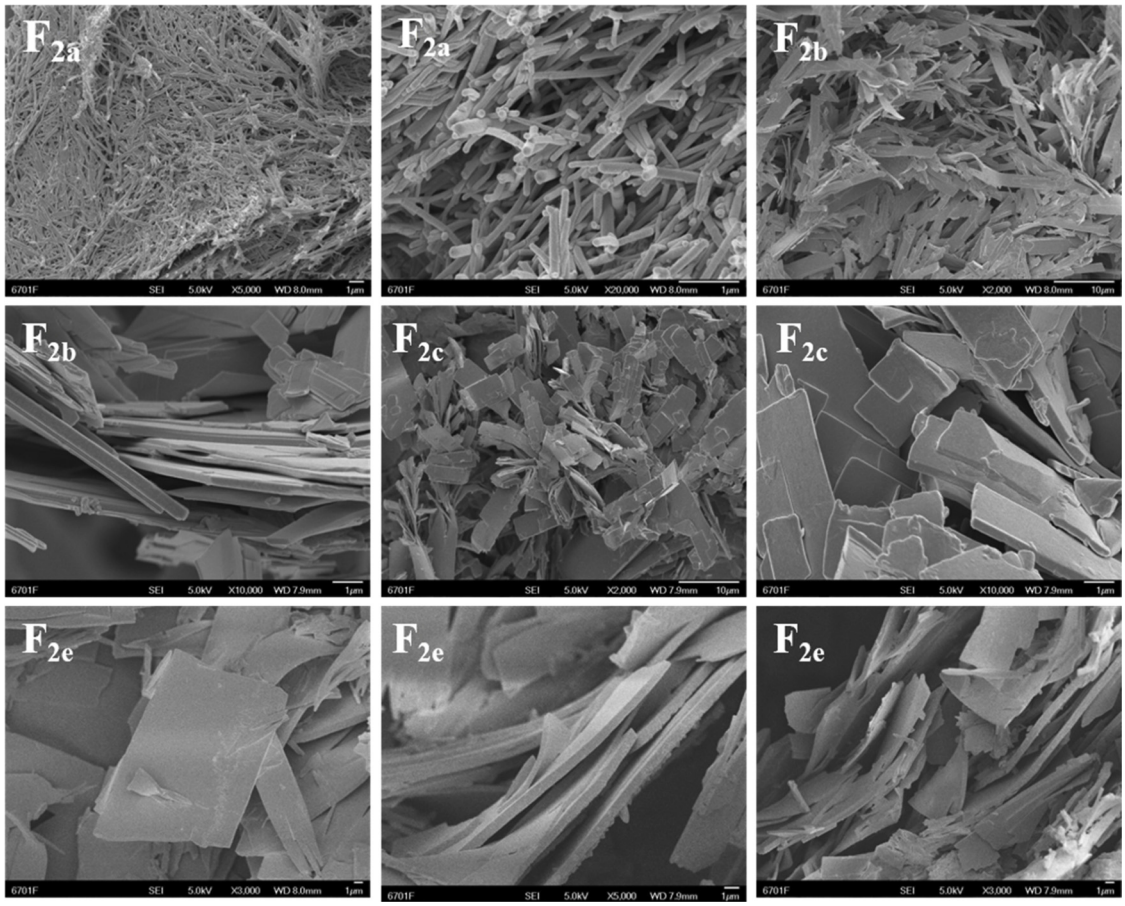

Fig. 7. SEM image of Chalcone gel molecule $F_{2a\text{-}2c}$ and F_{2e} xerogel.

is a structure similar to a crystalline state. It has been shown that for the same substituent, the longer the alkyl chain is, the more likely it is to form a sheet structure. The microstructure of F_{2e}-*iso*-propanol xerogel is lamellar, and it can be clearly seen when it is magnified 5000 times, layered structures that are intertwined to form a fiber network backbone through which the solvent is encapsulated to form a gel.

3.8. Self-assembly of chalcone gel molecules

Through FT-IR, XRD test and characterization, it is found that the gel molecule $F_{2a\text{-}2c}$ and F_{2e} were formed by self-assembly in an organic solvent through intermolecular hydrogen bonding, π-π stacking and van der Waals interaction. It is concluded by SEM that the F_{2a} forms a micron-scale rod-like structure in cyclohexane solvent; the gel molecule F_{2b} forms a regular band structure in *tert*-butanol; the gel molecule F_{2c} tends to form a lamellar structure in isooctane solvent and the gel molecule F_{2e} tends to form a layered structure in isopropanol solvent. As shown in Fig. 8, we boldly speculated on the self-assembly test of the gel molecule $F_{2a\text{-}2c}$ and F_{2e}.

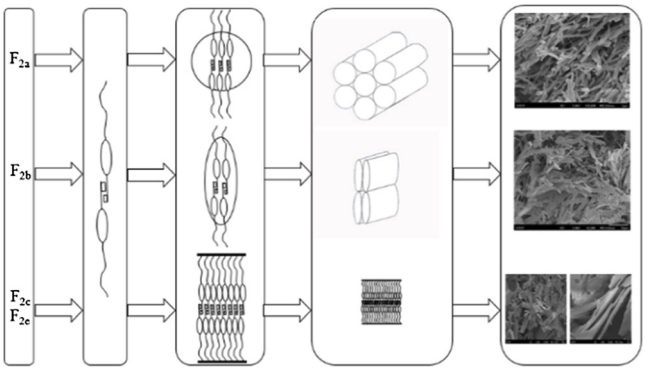

Fig. 8. Self-assembly method for gel molecules $F_{2a\text{-}2c}$ and F_{2e}.

4. Conclusion

In summary, five potential chalcone gels were designed and synthesized. Gelation tests in various solvents have shown that the difference in alkyl chain length associated with chalcone also plays an important role in gelation behavior. Under identical concentrations increasing the length of alkyl chains of the gel molecules and then the gel-to-sol transition temperature value is increased too. In addition, studies on the morphology of xerogels have shown that organogels are all composed of lamellar fiber structures. Based on FT-IR and XRD characterization and our discussion, mechanisms for forming organogels have been proposed. This research provides useful insights into the development and design of supramolecular soft materials.

Declaration of Competing Interest

The authors declare no competing interests.

Appendix A. Supplementary data

Supplementary material related to this article can be found, in the online version, at doi:https://doi.org/10.1016/j.colsurfa.2019.06.010.

The ^{1}H NMR and ^{13}C NMR of the intermediates M_1、H_1、H_2 and the gel molecules $F_{2a\text{-}2e}$ are detailed in the Supporting information. These materials are available free of charge via the Internet.

References

[1] B. Sukumaran Santhosh, V.K. Praveen, A. Ayyappanpillai, Functional π-gelators and their applications, Chem. Rev. 114 (2014) 1973–2129.
[2] P. Terech, R.G. Weiss, Low molecular mass gelators of organic liquids and the properties of their gels, Chem. Rev. 97 (1997) 3133–3160.
[3] D.J. Abdallah, R.G. Weiss, Organogels and low molecular mass organic gelators, Adv. Mater. 12 (2000) 1237–1247.
[4] J.W. Steed, Supramolecular gel chemistry: developments over the last decade, Chem. Commun. 47 (2011) 1379–1383.
[5] L.E. Buerkle, S.J. Rowan, Supramolecular gels formed from multi-component low molecular weight species, Chem. Soc. Rev. 41 (2012) 6089–6102.
[6] N.M. Sangeetha, M. Uday, Supramolecular gels: functions and uses, Chem. Soc. Rev. 34 (2005) 821–836.
[7] X. Cao, Q. Ding, Y. Li, A. Gao, X. Chang, Continuous multi-channel sensing of volatile acid and organic amine gases using a fluorescent self-assembly system, J. Mater. Chem. C Mater. Opt. Electron. Devices 7 (2018) 133–142.
[8] X. Cao, N. Zhao, A. Gao, Q. Ding, Y. Li, X. Chang, Terminal molecular isomer-effect on supramolecular self-assembly system based on naphthalimide derivative and its sensing application for mercury(II) and Iron (III) ions, Langmuir 34 (2018) 7404–7415.
[9] L. Jing, P. He, J. Yan, X. Fang, J. Peng, K. Liu, F. Yu, An organometallic super--gelator with multiple-stimulus responsive properties, Adv. Mater. 20 (2010) 2508–2511.
[10] C. Qun, L. Yuxia, Z. Deqing, Z. Guanxin, L. Chenyang, Z. Daoben, Cysteine and pH-responsive hydrogel based on a saccharide derivative with an aldehyde group, Langmuir 26 (2010) 3165–3168.
[11] V. Praveen Kumar, L. Jun, J. George, Enzyme catalysis: tool to make and break amygdalin hydrogelators from renewable resources: a delivery model for hydrophobic drugs, J. Am. Chem. Soc. 128 (2006) 8932–8938.
[12] A. Bimalendu, B. Arindam, Short-peptide-based hydrogel: a template for the in situ synthesis of fluorescent silver nanoclusters by using sunlight, Chem. Eur. J. 16 (2010) 13698–13705.
[13] X. Yang, G. Zhang, D. Zhang, Stimuli responsive gels based on low molecular weight gelators, J. Mater. Chem. 22 (2011) 38–50.
[14] S. Fran Ois-Xavier, N.S. Khelfallah, S. Marc, D. Nancy, P.J. Mésini, Formation of helical mesopores in organic polymer matrices, J. Am. Chem. Soc. 129 (2007) 3788–3789.
[15] R.J.H. Hafkamp, B.P.A. Kokke, I.M. Danke, H.P.M. Geurts, R.J.M. Nolte, Organogel formation and molecular imprinting by functionalized gluconamides and their metal complexes, Chem. Commun. 6 (1997) 545–546.
[16] T. Grace, S. Mohit, H. Jibao, V.T. John, G.L. Mcpherson, Use of a self-assembling organogel as a reverse template in the preparation of imprinted porous polymer films, Langmuir 21 (2005) 9322–9326.
[17] K.J.C.V. Bommel, F. Arianna, S. Seiji, Organic templates for the generation of inorganic materials, Angew. Chem. Int. Ed. Engl. 42 (2003) 980–999.
[18] S. Murdan, 1st meeting on topical drug delivery to the nail, Expert Opin. Drug Deliv. 4 (2007) 453–455.
[19] S. Murdan, T. Andrýsek, D. Son, Novel gels and their dispersions-oral drug delivery systems for ciclosporin, Int. J. Pharm. 300 (2005) 113–124.
[20] B.A. Kumar, R.R. Nayak, Studies on hydroquinone based maleate bolaamphiphile organogels and their drug formulations, Soft Matter (2018) 108–116.
[21] T.A. Khattab, B.D.B. Tiu, S. Adas, S.D. Bunge, R.C. Advincula, pH triggered smart organogel from DCDHF-Hydrazone molecular switch, Dyes Pigm. 130 (2016) 327–336.
[22] T.A. Khattab, B.D.B. Tiu, S. Adas, S.D. Bunge, R. Advincula, Solvatochromic, thermochromic and pH-sensory DCDHF-hydrazone molecular switch: response to alkaline analytes, RSC Adv. 6 (2016) 102296–102305.
[23] J. Puigmartí-Luis, V. Laukhin, D.P.A. Pérez, J. Vidal-Gancedo, C. Rovira, E. Laukhina, D.B. Amabilino, Supramolecular conducting nanowires from organogels, Angew. Chem. Int. Ed. Engl. 46 (2010) 238–241.
[24] M. Mohammad, P.R. Sundararajan, Low molecular weight organogels based on long-chain carbamates, Langmuir 21 (2005) 3802–3807.
[25] N.M. Sangeetha, M. Uday, Supramolecular gels: functions and uses, Chem. Soc. Rev. 34 (2005) 821–836.
[26] M. Hisashi, M. Toshio, A. Shin, T. Iwao, Y. Masayuki, Structural requirements of flavonoids for nitric oxide production inhibitory activity and mechanism of action, Bioorg. Med. Chem. 11 (2003) 1995–2000.
[27] H.H. Ko, L.T. Tsao, K.L. Yu, C.T. Liu, J.P. Wang, C.N. Lin, Structure–activity relationship studies on chalcone derivatives: the potent inhibition of chemical mediators release, Bioorg. Med. Chem. Lett. 11 (2003) 105–111.
[28] K.L. Lahtchev, D.I. Batovskab, V.M. Ubiyvovk, A.A. Sibirny, Antifungal activity of chalcones: a mechanistic study using various yeast strains, Eur. J. Med. Chem. 43 (2008) 2220–2228.
[29] Y. Qian, H.J. Zhang, P.C. Lv, H.L. Zhu, Synthesis, molecular modeling and biological evaluation of guanidine derivatives as novel antitubulin agents, Bioorg. Med. Chem. 18 (2010) 4310–4316.
[30] A. Lopez, D.G. Ming, Antifungal activity of benzoic acid derivatives from Piperlanceaefolium, J. Nat. Prod. 65 (2002) 62–64.
[31] K.L. Lahtchev, D.I. Batovskab, V.M. Ubiyvovk, A.A. Sibirny, Antifungal activity of chalcones: a mechanistic study using various yeast strains, Eur. J. Med. Chem. 43 (2008) 2220–2228.
[32] J.N. Domínguez, C. León, J. Rodrigues, D.D.N. Gamboa, J. Gut, P.J. Rosenthal, Synthesis and evaluation of new antimalarial phenylurenyl chalcone derivatives, J. Med. Chem. 48 (2005) 3654–3658.
[33] K.V. Sashidhara, G.R. Palnati, R. Sonkar, S.R. Avula, C. Awasthi, G. Bhatia, Coumarin chalcone fibrates: a new structural class of lipid lowering agents, Eur. J. Med. Chem. 64 (2013) 422–431.
[34] K. Nakagawa-Goto, P.C. Wu, K.F. Bastow, S.C. Yang, S.L. Yu, H.Y. Chen, J.C. Lin, M. Goto, S.L. Morris-Natschke, P.C. Yang, Antitumor agents 283. Further elaboration of Desmosdumotin C analogs as potent antitumor agents: activation of spindle assembly checkpoint as possible mode of action, Bioorg. Med. Chem. 19 (2011) 1816–1822.
[35] P.C. Leow, P. Bahety, C.P. Boon, Y.L. Chong, K.L. Tan, T. Yang, P.L.R. Ee, Functionalized curcumin analogs as potent modulators of the Wnt/β-catenin signaling pathway, Eur. J. Med. Chem. 71 (2014) 67–80.
[36] S. Vogel, J. Heilmann, Synthesis, cytotoxicity, and antioxidative activity of minor prenylated chalcones from Humulus lupulus, J. Nat. Prod. 71 (2008) 1237–1241.
[37] S. Vogel, M. Barbic, G. Jürgenliemk, J. Heilmann, Synthesis, cytotoxicity, antioxidative and anti-inflammatory activity of chalcones and influence of A-ring modifications on the pharmacological effect, Eur. J. Med. Chem. 45 (2010) 2206–2213.
[38] D. Sylvie, The development of chalcones as promising anticancer agents, Idrugs Invest. Drugs J. 10 (2007) 42–46.
[39] A. Dhiman, A. Nanda, S. Ahmad, A quest for staunch effects of flavonoids: utopian protection against hepatic ailments, Arab. J. Chem. 12 (2012) 1702–1711.
[40] O.J.B. And, Neil Osheroff, Bioflavonoids as poisons of human topoisomerase IIα and IIβ, Biochemistry 46 (2007) 6097–6108.
[41] D. Kim, J. Park, J. Kim, C. Han, J. Yoon, N. Kim, J. Seo, C. Lee, Flavonoids as mushroom tyrosinase inhibitors: a fluorescence quenching study, J. Agric. Food Chem. 54 (2006) 935–941.
[42] A.L. Simons, M. Renouf, A. Suzanne Hendrich, P.A. Murphy, Human gut microbial degradation of flavonoids: structure − function relationships, J. Agric. Food Chem. 53 (2005) 4258–4263.
[43] L.J. Ha, L.J. Hyeok, J. Sung Ho, H. Tae Kyung, F. Mingxiao, K. Jae-Yean, L. Jae-Hong, L. Hoyeon, K. Jong Seung, K. Chulhun, Highly selective fluorescence imaging of zinc distribution in HeLa cells and Arabidopsis using a naphthalene-based fluorescent probe, Chem. Commun. 51 (2015) 7463–7465.
[44] G.S. Lim, B.M. Jung, S.J. Lee, H.H. Song, Y.C. Ji, Synthesis of polycatenar-type organogelators based on chalcone and study of their supramolecular architectures, Chem. Mater. 19 (2007) 460–467.
[45] X. Yang, G. Zhang, D. Zhang, Stimuli responsive gels based on low molecular weight gelators, J. Mater. Chem. 22 (2011) 38–50.